Viral targeting of fibroblastic reticular cells contributes to immunosuppression and persistence during chronic infection

Scott N. Mueller*, Mehrdad Matloubian†, Daniel M. Clemens‡, Arlene H. Sharpe§, Gordon J. Freeman¶‖, Shivaprakash Gangappa**, Christian P. Larsen**, and Rafi Ahmed*††

*Emory Vaccine Center and Department of Microbiology and Immunology, Emory University, Atlanta, GA 30322; †Department of Medicine, Division of Rheumatology, University of California, San Francisco, CA 94143; ‡Department of Medicine, Division of Infectious Diseases, University of California, Los Angeles, CA 90095; §Department of Pathology, Harvard Medical School and Brigham and Women's Hospital, Boston, MA 02115; ¶Department of Medical Oncology, Dana–Farber Cancer Institute, Boston, MA 02115; ‖Department of Medicine, Harvard Medical School, Boston, MA 02115; and **Emory Transplant Center and Department of Surgery, Emory University School of Medicine, Atlanta, GA 30322

Edited by James P. Allison, Memorial Sloan–Kettering Cancer Center, New York, NY, and approved August 10, 2007 (received for review March 19, 2007)

Many chronic viral infections are marked by pathogen persistence and a generalized immunosuppression. The exact mechanisms by which this occurs are still unknown. Using a mouse model of persistent lymphocytic choriomeningitis virus (LCMV) infection, we demonstrate viral targeting of fibroblastic reticular cells (FRC) in the lymphoid organs. The FRC stromal networks are critical for proper lymphoid architecture and function. High numbers of FRC were infected by LCMV clone 13, which causes a chronic infection, whereas few were infected by the acute strain, LCMV Armstrong. The function of the FRC conduit network was altered after clone 13 infection by the action of CD8$^+$ T cells. Importantly, expression of the inhibitory programmed death ligand 1, which was up-regulated on FRC after infection, reduced early CD8$^+$ T cell-mediated immunopathology and prevented destruction of the FRC architecture in the spleen. Together, this reveals an important tropism during a persistent viral infection. These data also suggest that the inhibitory PD-1 pathway, which likely evolved to prevent excessive immunopathology, may contribute to viral persistence in FRC during chronic infection.

immunopathology | stromal cells | viral infection

Many acute and chronic viral infections induce a generalized immunosuppression (1, 2). This suppression of immunity is often transient, occurring during the acute phase of infection; however, prolonged suppression can also occur during certain chronic viral infections. The mechanisms of virus-induced immunosuppression are complex and varied (1–3). Infection of mice with lymphocytic choriomeningitis virus (LCMV) is a useful model to dissect the mechanisms of viral persistence and immunosuppression. The clone 13 (CL-13) strain of LCMV results in a chronic infection in adult mice, marked by persisting virus and a generalized immunosuppression. Viral load rises rapidly within days and remains high over a prolonged period, suppressing specific immunity by inducing an hierarchical loss of CD8$^+$ T cell function (4, 5). This CL-13 chronic infection is also associated with increased susceptibility to opportunistic secondary infections (6–8).

Chronic LCMV infection results in reduced cellularity and altered splenic architecture (9). Enhanced infection of dendritic cells (DC), resulting in reduced T cell stimulatory capacity and destruction of the DC, has been proposed as one mechanism by which CL-13 initiates immunosuppression within the host (8, 10). Although DC in the spleen can be infected by LCMV CL-13, this represents a relatively small proportion of total infected cells. It follows that other cell types are infected by CL-13 and likely contribute to the pronounced immunosuppression and architectural disruption of lymphoid organs that are observed after infection.

Through a detailed kinetic examination of the cell types infected during LCMV CL-13 infection we discovered that fibroblastic reticular cells (FRC) are an important target of infection by this virus. Secondary lymphoid tissues are supported by a complex microarchitecture of reticular fibers surrounded by FRC, which provide a three-dimensional framework on which immune cells travel (11, 12). In addition, chemokines involved in lymphocyte homing (such as CCL21 and CCL19) are expressed by the FRC in secondary lymphoid tissues (13). Thus, lymphocyte migration, recruitment, and activation are efficiently regulated by the FRC network. In this report we demonstrate that widespread infection of the FRC resulted in disruption of FRC conduit function. Importantly, early immunopathology was markedly reduced via the involvement of the inhibitory programmed death 1 [PD-1/PD ligand 1 (PD-L1)] pathway. These findings demonstrate that FRC cells are a significant target of LCMV CL-13 infection and contribute to viral burden and persistence during chronic infection.

Results

LCMV CL-13 Infects FRC. LCMV Armstrong and CL-13 are responsible for very different outcomes of infection in adult mice: acute and chronic infections, respectively. Clearance of Armstrong occurs within 1 week of infection, coinciding with a large specific T cell response. Conversely, CL-13 persists at high titers in blood and tissues for several months, resulting in functional exhaustion of virus-specific T cells and a generalized immune suppression. Although CL-13 can infect DC (10), other additional mechanisms may also play a role in the functional impairment of the responding T cells (14). Assessment of viral antigen distribution in the spleen after CL-13 infection revealed a distinctly different localization in comparison with LCMV Armstrong infection. Armstrong largely localized to the marginal zones (Fig. 1*A*), with minor staining within white pulp (WP) and red pulp (RP). In contrast, CL-13 was found in the marginal zones and extensively throughout the WP and also in the RP. Moreover, a distinctly reticular pattern of LCMV antigen was apparent throughout the WP after CL-13 infection, suggesting potential infection of the lymphoid stroma.

Author contributions: S.N.M., M.M., and R.A. designed research; S.N.M., M.M., and D.M.C. performed research; A.H.S., G.J.F., S.G., and C.P.L. contributed new reagents/analytic tools; S.N.M. analyzed data; and S.N.M. and R.A. wrote the paper.

The authors declare no conflict of interest.

This article is a PNAS Direct Submission.

Abbreviations: LCMV, lymphocytic choriomeningitis virus; CL-13, clone 13; PD, programmed death; PD-L1, PD ligand 1; FRC, fibroblastic reticular cell; WP, white pulp; RP, red pulp; LN, lymph node; DC, dendritic cell.

††To whom correspondence should be addressed. E-mail: ra@microbio.emory.edu.

This article contains supporting information online at www.pnas.org/cgi/content/full/0702579104/DC1.

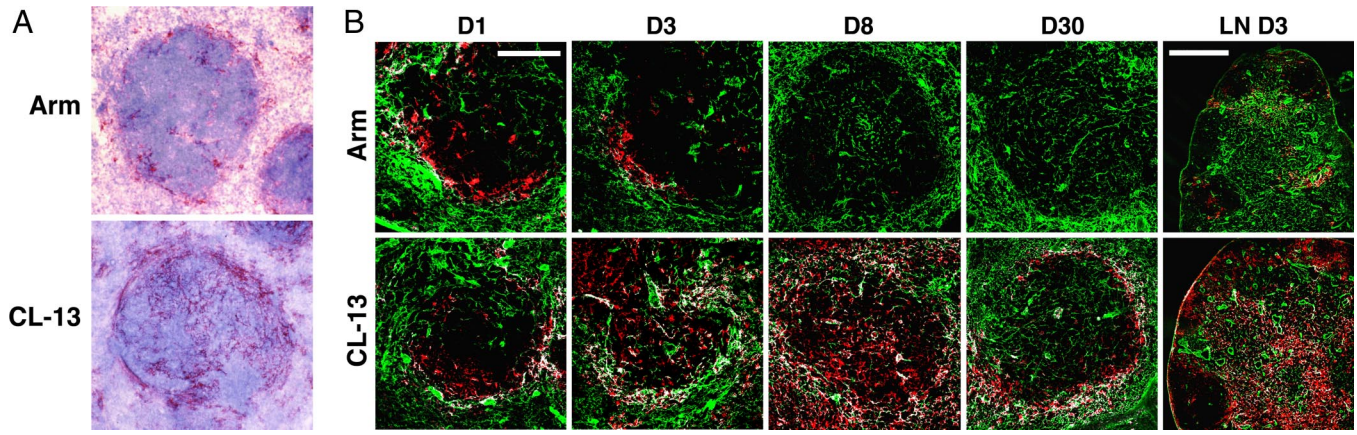

Fig. 1. Reticular pattern of virus infection in the spleen after CL-13 infection. (*A*) Spleens from mice infected with LCMV Armstrong (Arm) or CL-13 3 days earlier were stained for LCMV antigen, counterstained with Mayer's hematoxylin, and examined via microscopy. (*B*) Spleens and LN (*Right*) stained for ER-TR7 (green) and LCMV (red) on days 1–30 after infection. White regions indicate colocalization. [Magnification: ×20 (spleen) and ×10 (LN). Scale bars: 100 μm (spleen) and 400 μm (LN).]

To visualize cells of the reticular network, we used the monoclonal antibody ER-TR7 (15), which stains the network of FRC in the WP and RP [supporting information (SI) Fig. 6]. Detailed examination of WP FRC was also performed by staining for laminin, smooth muscle actin, and desmin, as well as the collagen III$^+$ reticular fibers ensheathed by the FRC (16) (SI Fig. 6).

To determine whether LCMV CL-13 was infecting stromal cells we performed a kinetic analysis of viral infection in the spleen. Spleens were harvested between 1 and 30 days after infection and costained for LCMV and ER-TR7 antigens. Initially (day 1), both in mice infected with LCMV Armstrong and in mice infected with CL-13, virus predominantly localized to the marginal zone (Fig. 1*B*). At this point, the degree of cellular infection appeared to be very similar between the two strains. Within 3 days of infection, however, CL-13 could be observed throughout the WP and more extensively in the RP. Infection of both the WP and RP by CL-13 further increased, peaking at day 8 and remaining high for at least 30 days after infection. In stark contrast, Armstrong infection remained mostly localized to the marginal zone and was controlled by day 8. Importantly, LCMV antigen appeared to colocalize with ER-TR7$^+$ FRC after CL-13, but not Armstrong, infection. Indeed, a substantial proportion of the infected cells after CL-13 infection appeared to correspond to cells of the reticular network.

A closer look at infection of splenocytes after Armstrong infection revealed large cells of distinct morphology staining positive for LCMV (Fig. 2*A*). Macrophages were infected by both Armstrong and CL-13, yet neither strain was observed to infect T or B lymphocytes (data not shown). Whereas very few FRC were positive for viral antigen in Armstrong-infected spleens, many were heavily infected within just 3 days of CL-13 infection. Furthermore, colocalization of LCMV antigen with collagen III, laminin, smooth muscle actin, and desmin was used to clearly determine infection of the FRC by LCMV CL-13 (Fig. 2*B*). Laminin$^+$ ER-TR7$^-$ cells in the B cell zones were also found to colocalize with LCMV, suggesting that these stromal cells may also be a target of LCMV CL-13 infection (data not shown).

Given the systemic nature of LCMV infection, we also examined peripheral lymph nodes (LN) for the presence of LCMV antigen-positive FRC. Similar to the pattern of infection in the spleen, LCMV antigens were observed in LN FRC after CL-13 infection (Figs. 1*B* and 2*A*). Minimal infection of FRC was observed in the LN during Armstrong infection.

Infection of the FRC by CL-13 was determined by transmission electron microscopy. Staining for LCMV antigen revealed highly infected reticular cells and cell processes ensheathing bundles of collagen fibers (Fig. 2*C*). Lymphocytes observed in close association with the FRC were not infected. Infected reticular cells did not express MHC class II or Fc receptors (SI Fig. 7). Lastly, infection of FRC was quantified by flow cytometry after dissociation of the spleen by collagenase treatment (Fig. 2*D*). Almost two-thirds of ER-TR7$^+$ cells isolated from the spleen stained positive for LCMV antigen after CL-13 infection. This was in contrast to only 6.6 ± 2.8% of CD11c$^+$ DC that were found to be infected with LCMV at this time. Together, these data demonstrate that LCMV CL-13 targets reticular stromal cells in the lymphoid tissues.

We examined the genetic basis of CL-13 FRC tropism using reassortants of the Armstrong and CL-13 viruses. The LCMV genome consists of two single-stranded RNA segments designated large (L) and small (S), which encode the viral polymerase protein and the glycoprotein, respectively. LCMV CL-13 differs by only two amino acids from the parent strain, LCMV Armstrong (17). These have been mapped to a single amino acid change in the viral polymerase that may increase viral yield within infected cells and a single change in the glycoprotein that is important in determining the degree of infectivity (18, 19). We infected mice with viruses containing the L segment from CL-13 and the S segment from Armstrong (13/Arm) or vice versa (Arm/13). Mice infected with either reassortant virus displayed large numbers of infected cells and infected FRC (SI Fig. 8). However, neither reassortant demonstrated a pattern of infection equivalent to that of CL-13, which appeared to infect greater numbers of cells in the spleen. Thus, mutations in both the polymerase and glycoprotein genes of LCMV CL-13 appeared to contribute to the tropism exhibited by the virus.

Disruption of the Conduit Network During CL-13 Infection. The stromal network is thought to play numerous roles in lymphoid organs, influencing cell recruitment, migration, activation, and survival through organization of the lymphoid cellular and molecular microarchitecture. The FRC form a contiguous network of conduits that allow transport of small molecules and antigens directly into the T zones without perfusing through the parenchyma (20). CL-13 infection is characterized by disruption of the lymphoid architecture, including smaller, disorganized

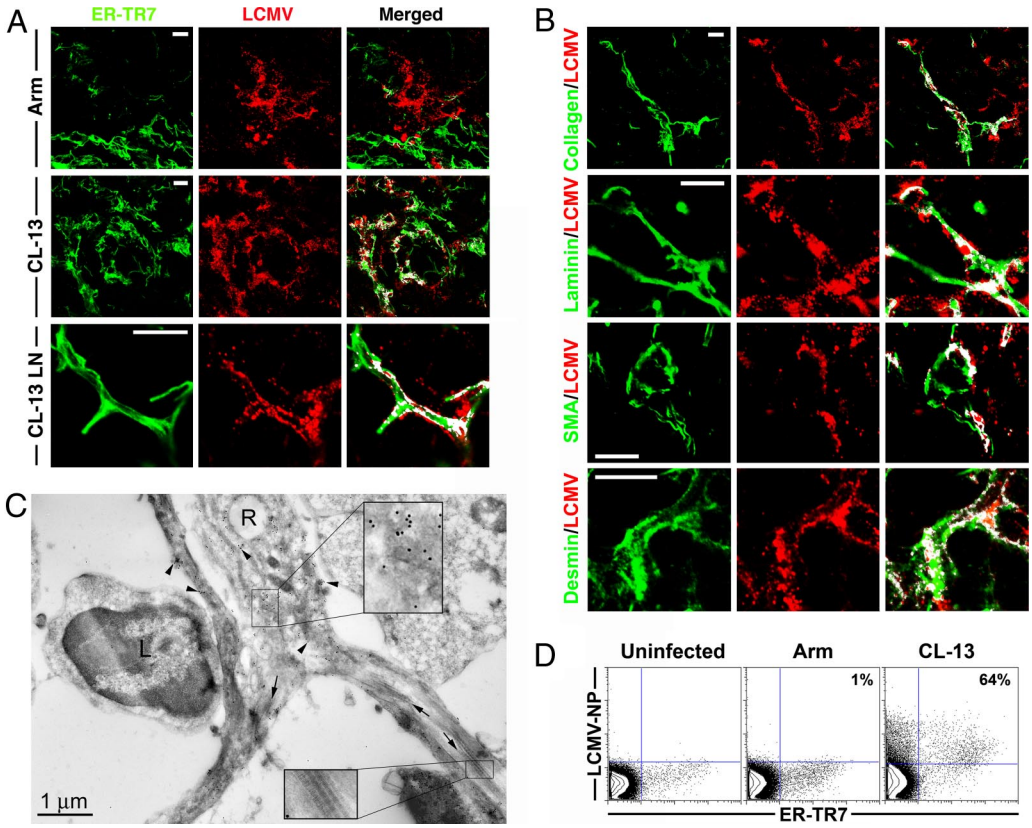

Fig. 2. LCMV CL-13 infects FRC. (*A*) ER-TR7$^+$ cells colocalized with LCMV antigen 3 days after Arm infection in the spleen, or CL-13 infection in the spleen and LN. (*B*) Colocalization of LCMV antigen with FRC components collagen III, laminin, smooth muscle actin, and desmin. White regions indicate colocalization in merged images. (Magnification: ×100. Scale bars: 10 μm.) (*C*) Spleen sections 3 days after CL-13 infection analyzed by electron microscopy. A reticular cell (R) from the WP reveals concentrated deposits of LCMV antigen (15-nm gold particles, arrowheads), magnified in *Upper Inset*. Reticular cell processes surround the reticular fibers (arrows), which are composed of bundles of collagen (magnified in *Lower Inset*). An uninfected lymphocyte (L) can be observed interacting with the infected reticular cell. (*D*) FRC isolated from spleens 8 days after infection with CL-13 or Arm were stained for ER-TR7 and LCMV antigen. Numbers represent the percentage of ER-TR7$^+$ cells staining positive for LCMV nucleoprotein.

WP regions and reduced cellularity within the WP. Infected FRC may die, lose cellular integrity, or experience disruption of cell–cell contacts that keep the conduit lumen separate from the splenic parenchyma. To examine the integrity of the conduit network after LCMV infection, mice were injected intravenously with fluorescently labeled tracer molecules (Fig. 3*A*). Small molecules accumulate within the conduit network in the spleen after injection (21), making it possible to trace the functional

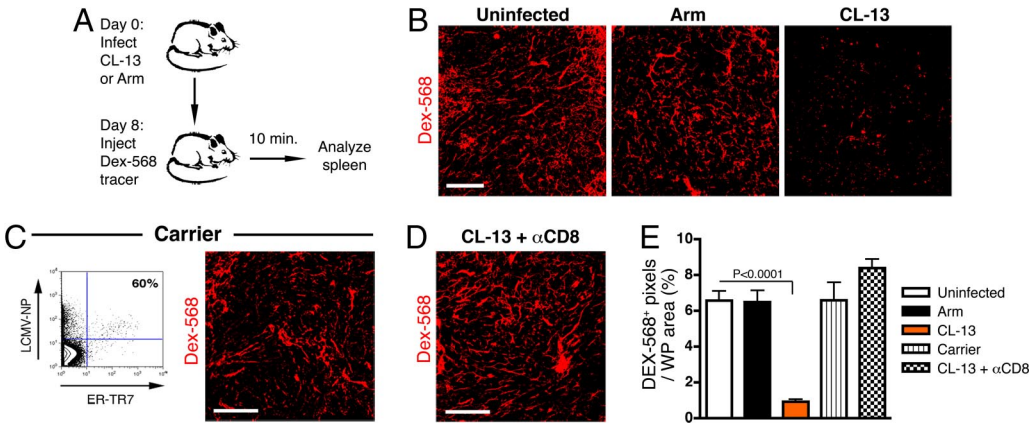

Fig. 3. Impaired FRC conduit function after LCMV CL-13 infection. (*A*) Mice infected with LCMV Arm or CL-13 8 days previously were injected intravenously with dextran Alexa Fluor 568 tracer (Dex-568). Spleens were removed after 10 min and immediately fixed. (*B*) Localization of Dex-568 tracer within the conduit network of the splenic WP. (*C*) Infected FRC in carrier mice stained with ER-TR7 and LCMV nucleoprotein antibodies after isolation by collagenase treatment from spleen. Shown is accumulation of Dex-568 in the conduits of the spleens of carrier mice. Spleens were analyzed as described in *A*. (*D*) Tracer accumulation in mice treated with anti-CD8 antibodies and infected with CL-13 (day 8). (Scale bars: 100 μm.) (*E*) Quantitation of Dex-568$^+$ pixels as a proportion of WP area in the spleen.

framework of the conduit network. In uninfected (control) mice, Alexa Fluor 568-conjugated dextran (Fig. 3*B*) and OVA-FITC (data not shown) were clearly observed in the conduits of the spleen 10 min after injection. In mice infected with LCMV Armstrong, greater amounts of tracer accumulated within the marginal sinuses (data not shown); however, the tracers were found to accumulate within the conduits, similar to that in uninfected mice. In contrast, during CL-13 infection there was marked disruption in the ability of the tracers to accumulate within the conduit network in the WP of the spleen. We observed an ≈86% and ≈74.5% reduction in Dex-568 or OVA-FITC tracer accumulation, respectively, in WP areas after CL-13 infection when compared with uninfected mice (Fig. 3*E* and data not shown). Tracer could be found in association with some cells in the RP, possibly because of leakage into the splenic parenchyma and association with resident cells. These data suggest that LCMV CL-13 infection is detrimental to the function of the FRC conduit network in the spleen.

CD8$^+$ T Cell Involvement in Disruption of the Conduit Network. The altered drainage of antigen in the conduit networks in mice infected with LCMV CL-13 may have resulted from damage due to direct infection of the FRC or immune-mediated damage. Although LCMV is a noncytolytic virus, infection of cells is known to have detrimental effects on the health, or the "luxury functions," of the cells it infects (22). Such an alteration in function may account for the disrupted FRC function. We examined carrier mice infected with LCMV CL-13 *in utero*, which are immunologically tolerant to the virus because of deletion of virus-specific T cells and display no generalized virus-induced immunosuppression. Carrier mice were found to have entirely normal splenic conduit drainage despite large numbers of infected FRC (Fig. 3 *C* and *E*). This suggested that aspects of the immune response were responsible for disruption of tracer drainage in CL-13-infected mice.

To examine the role of CD8$^+$ T cells in damage to the conduit network during CL-13 infection, mice were depleted of CD8$^+$ T cells before infection. In these mice, accumulation of tracer molecules was similar to that in uninfected mice (Fig. 3 *D* and *E*). This corresponded with the reduced disruption of the lymphoid architecture and increased cellularity observed during chronic LCMV infection in mice depleted of CD8$^+$ T cells (data not shown) (9). Mice deficient in perforin and IFN-γ showed improved tracer accumulation in the WP after CL-13 infection when compared with WT mice (SI Fig. 9). However, neither knockout strain demonstrated levels of tracer accumulation comparable to uninfected mice, indicating that both cytotoxicity and cytokine production play a role in disruption of the conduits during CL-13 infection. Together, these data suggest that the integrity of the conduit network may be disrupted by responding CD8$^+$ T cells during CL-13 infection, either preventing molecules from entering the network or allowing them to escape from the conduit lumen and perfuse into the splenic parenchyma.

FRC Express High Levels of PD-L1 During LCMV Infection. Despite infection of significant numbers of FRC by LCMV CL-13 and immune-mediated disruption of conduit function, the complex network of FRC was not obviously killed or depleted from the spleen during infection. This suggested that the FRC may use mechanisms that protect them from T cell-mediated death. We recently demonstrated that one of the major mechanisms involved in the impairment of T cell function during LCMV CL-13 infection involves up-regulation of the molecule PD-1 on T cells (23). Interaction of this inhibitory receptor with its ligand PD-L1 directly influences T cell responses. PD-L1 is widely expressed on cells such as macrophages, DC, T and B cells, Kupffer cells in the liver, and β cells in the pancreas, among others (24). We examined expression of PD-L1 on FRC isolated from the spleen.

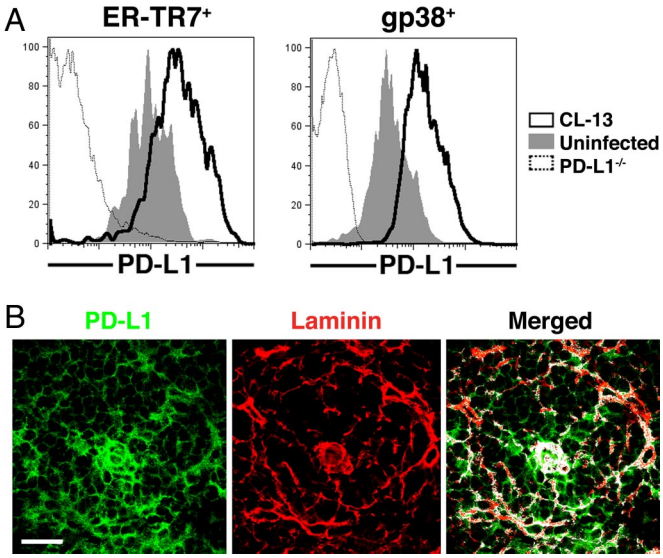

Fig. 4. PD-L1 expression by FRC. (*A*) FRC were isolated from the spleens of uninfected or day-6 CL-13-infected mice and stained with ER-TR7 or anti-gp38 and anti-PD-L1 antibodies. PD-L1 expression was determined on gated ER-TR7$^+$ or gp38$^+$ cells from uninfected (solid histogram) or CL-13-infected (black line) mice. PD-L1$^{-/-}$ mice were used for negative PD-L1 expression (dotted line). (*B*) Spleens from mice infected with CL-13 6 days previously were stained for PD-L1 (green) and laminin (red) and analyzed via confocal microscopy. White regions indicate colocalization. (Magnification: ×63. Scale bar: 25 μm.)

The ER-TR7$^+$ FRC were found to constitutively express PD-L1 and up-regulated the inhibitory ligand considerably after LCMV CL-13 infection (Fig. 4*A*). Up-regulation of PD-L1 expression of FRC was confirmed by staining the cells for gp38, a surface marker found on the lymphoid reticular cells (25). When spleen sections were examined via microscopy, high levels of PD-L1 were observed on the FRC in CL-13-infected mice (Fig. 4*B*). This suggested that PD-L1-expressing FRC in the lymphoid tissues may play a role in regulating the function of PD-1-expressing virus-specific T cells during chronic LCMV infection and that this inhibitory interaction (PD-1/PD-L1) may protect the FRC from being killed.

PD-L1 Blockade Induces Severe Immunopathology in Lymphoid FRC. We recently demonstrated that blockade of the PD-1/PD-L1 inhibitory pathway can restore function in exhausted CD8$^+$ T cells during chronic CL-13 infection (23). Given that PD-L1 was highly expressed on FRC during the early stage of CL-13 infection, we sought to examine the role for this expression by treating mice with anti-PD-L1 antibody (Fig. 5*A*). Two days after treatment, mice exhibited severe immunopathology in the spleen. In particular, mice treated with anti-PD-L1 antibody displayed noticeably increased disruption of the splenic stromal architecture (Fig. 5*B*). This included smaller WP regions and considerable alteration to the ER-TR7$^+$ stromal network in the RP and WP. We found that ER-TR7 antigen was reduced by ≈54% (Fig. 5*C*) and appeared less uniform, indicative of loss or alteration of the stromal cells. Furthermore, PD-L1 blockade induced redistribution of viral antigen. Many large deposits of LCMV antigen were observed after treatment (Fig. 5*B*, arrows), suggesting possible uptake by phagocytic cells. As described above, no significant destruction or loss of the stromal network was detected in untreated CL-13-infected mice. Moreover, in mice lacking CD8$^+$ T cells, FRC immunopathology was not observed after anti-PD-L1 treatment: ER-TR7 antigen expression was similar to untreated mice, and the spleen architecture appeared relatively intact (Fig. 5 *B* and *C*). Together, these data

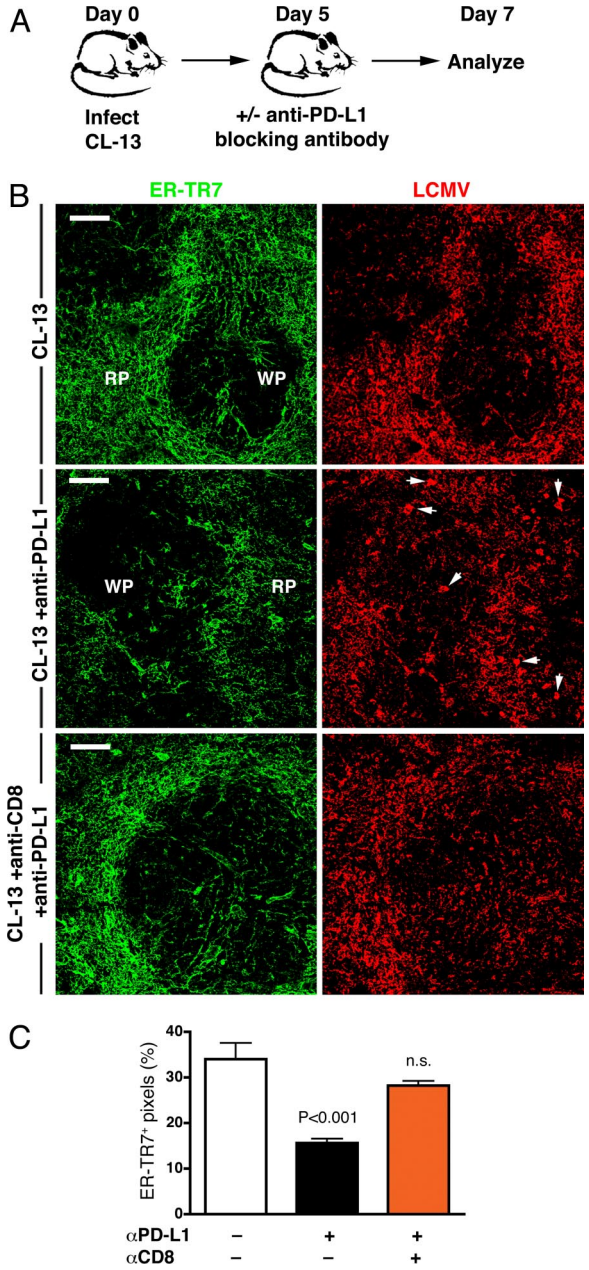

Fig. 5. Blockade of PD-L1 induces severe immunopathology. (*A*) Mice were infected with LCMV CL-13, treated with anti-PD-L1 blocking antibody on day 5, and analyzed 2 days later. (*B*) Spleens were stained for ER-TR7 (green) and LCMV (red) antigens and analyzed via microscopy. White arrows indicate examples of large deposits of LCMV antigen not observed in untreated mice. (Magnification: ×20. Scale bars: 100 μm.) (*C*) Assessment of FRC immunopathology was performed by quantitating ER-TR7$^+$ pixels in the spleens of mice after CL-13 infection and anti-PD-L1 treatment.

clearly demonstrate that PD-L1 expression prevents severe immunopathology and architectural disruption of the FRC network in the spleen, promoting persistence of LCMV CL-13 in infected lymphoid stromal cells.

Discussion

The lymphoid stromal cells have multiple important structural and functional roles in the control of immune responses (12, 20, 26, 27). We demonstrate here that FRC are a target during LCMV CL-13 infection. Importantly, infected stromal cells constituted a significant proportion of the virally infected cells in the spleen and thus greatly contributed to the overall viral burden. We also show that responding CD8$^+$ T cells altered the function of the FRC network yet were prevented from causing severe immunopathology early after infection because of expression of PD-L1 on FRC. Infection of FRC, particularly by pathogens that persist in a chronic state, may facilitate rapid spread and long-term survival of the virus in the host. From the hosts' perspective, however, damage to the large stromal network may be highly detrimental to ongoing and future immune responses.

To combat a rapidly replicating pathogen the immune system must respond with equally aggressive speed and specificity. Integral to this, antigen, antigen-presenting cells, and specific lymphocytes must come together in the lymphoid organs. Much of this may be facilitated by the surrounding reticular network, which forces close interaction between migrating T cells and local antigen-presenting cells (11, 28), enables the rapid transport and presentation of antigens through the FRC conduit network (20, 21, 26), and controls the recruitment and local migration of lymphocytes via presentation of chemokines (13). Targeting of FRC by LCMV CL-13 has potential consequences for the structural integrity of the reticular network and its overall function. Indeed, the drainage of tracer molecules through the network was impaired, as was the overall lymphoid architecture and cellularity in the spleens of CL-13-infected mice. Thus, alterations in the normal functions of the FRC may be an important mechanism by which LCMV induces immunosuppression.

The architectural disruption that occurs after CL-13 infection has been attributed to destruction of infected antigen-presenting cells, including DC, by CD8$^+$ T cells (9). Similarly, infection of endothelial cells and macrophages by murine cytomegalovirus has been linked to remodeling of the spleen (29). Because the reticular stromal network is critical for the overall architecture of the lymphoid organs, much of the architectural disruption may be attributed to effects on the stromal cells. The plasticity of the reticular network, particularly during infections (27), suggests that much damage to the network may be repaired rapidly and that the FRC may protect themselves from death by cells of the immune system. Our results demonstrate that PD-L1 expression can protect the FRC from being killed by activated PD-1$^+$ CD8$^+$ T cells, reducing lymphoid immunopathology during chronic viral infection. Blocking PD-L1 function via antibody treatment resulted in markedly greater disruption of the splenic architecture and redistribution of viral antigen, only when CD8 T cells were present.

Many chronic infections are characterized by high levels of persisting virus. Antigen levels, or the amount of antigen seen by responding T cells, may constitute one of the most important factors influencing functional T cell exhaustion (5). An important factor affecting viral load is the tropism of the pathogen. We show here that CL-13 targets the extensive FRC network in the lymphoid tissues. Although LCMV CL-13 also infects DC (10), this represents a relatively small number of infected cells in the lymphoid tissue, given that only 1–2% of total splenocytes are DC. The receptor for LCMV, α-dystroglycan, is highly expressed on stromal and epithelial cells in many different tissues (30), suggesting that these cells may constitute a significant antigen burden in tissues during CL-13 infection. Furthermore, we have found that antigen presentation by infected nonhematopoietic cells strongly influences the degree of T cell exhaustion and immunosuppression during CL-13 infection (S.N.M. and R.A., unpublished observations).

In summary, we demonstrate that infection and disruption of the extensive FRC network occur during LCMV CL-13 infection. Interestingly, FRC may also play a role in Ebola virus and HIV pathogenesis (31, 32). Importantly, we demonstrate that the PD-1 inhibitory pathway greatly reduced stromal immunopa-

thology and architectural disruption after infection. Hence, both the virus and the host may benefit from the PD-1 inhibitory pathway, which, by reducing immune pathology, may assist the virus to persist in infected stromal cells. This also suggests that the efficacy of PD-1-based therapies to restore immune function during chronic infections may be affected by tropism and the potential for immunopathologic damage by blocking the PD-1 pathway.

Materials and Methods

Infections. C57BL/6 mice were infected with 2×10^5 pfu of Armstrong or 2×10^6 pfu of CL-13 or the reassortant viruses Arm/13 and 13/Arm (18) intravenously. For a description of mouse strains used and antibody treatment see *SI Materials and Methods*.

Microscopy. For a description of standard immunohistochemistry and transmission electron microscopy methods used, see *SI Materials and Methods*. For immunofluorescence, spleens were removed from mice and frozen in TissueTek OCT (Sakura FineTek, Torrance, CA). Twenty-micrometer cryostat sections were fixed in ice-cold acetone for 10 min. Sections were stained with ER-TR7 (Biogenesis, Bournemouth, U.K.), anti-type III collagen (Southern Biotechnology Associates, Brimingham, AL), anti-laminin (AbD Serotec, Raleigh, NC), anti-α-smooth muscle actin (Sigma, St. Louis, MO), polyclonal rabbit anti-desmin (Monosan, Uden, The Netherlands), polyclonal anti-LCMV guinea pig serum, or anti-PD-L1 biotin (eBioscience, San Diego, CA). Stains were visualized with Alexa Fluor 488-, 568-, or 647-conjugated goat anti-rat, anti-hamster, anti-rabbit, or anti-guinea pig Ig (Invitrogen, Carlsbad, CA) and analyzed on an LSM510 confocal microscope (Zeiss Microimaging). Images were prepared in NIH ImageJ, with a colocalization plug-in, and compiled in Photoshop (Adobe Systems, San Jose, CA). Analysis of ER-TR7$^+$ antigen distribution after anti-PD-L1 treatment was performed by using ImageJ software and measurement functions to count ER-TR7$^+$ pixels as a proportion of tissue area (n = 5–10 mice per group).

Fluorescent Tracers. Ten-kilodalton lysine fixable dextran 568, OVA, and OVA-FITC (5 mg/ml) were purchased from Invitrogen. Tracers were injected intravenously in 200 μl of PBS, and mice were killed after 10 min. Spleens were immersion-fixed overnight in 4% paraformaldehyde, washed twice in PBS, and frozen in OCT. For quantitation of tracer-positive pixels per area of WP, spleens were analyzed by using NIH ImageJ software and built-in measurement functions (n = 14–22). Statistical analysis was performed by a two-tailed t test with 95% confidence intervals using Prism software (GraphPad).

Flow Cytometry. Spleens were prepared as described previously (33). Cells were fixed by using the Cytofix/Cytoperm kit (BD Biosciences, San Jose, CA) and stained intracellularly with ER-TR7 antibody and Alexa Fluor 488 goat anti-rat IgG (Invitrogen) and costained with anti-LCMV nucleoprotein antibody conjugated to Alexa Fluor 647. Alternately, cells were stained with phycoerythrin-conjugated anti-PD-L1 (eBioscience) before fixation, or with anti-gp38 antibody (25) and anti-PD-L1-biotin, followed by goat anti-Syrian hamster FITC and streptavidin–allophycocyanin (Invitrogen). Appropriate rat or Syrian hamster IgG isotype antibodies were used as controls. PD-L1$^{-/-}$ mice were used to control for PD-L1 staining. Samples were acquired by using a FACSCalibur flow cytometer (BD Biosciences).

We thank the Nusrat laboratory for use of their confocal microscope. This work was supported by the National Institutes of Health (Grant AI56299 to A.H.S., G.J.F., and R.A. and Grants AI30048 and AI04464409 to R.A.) and a grant from the Gates Foundation Grand Challenges in Global Health (to R.A.). S.N.M. was supported by a CJ Martin Overseas Biomedical Fellowship from the National Health and Medical Research Council of Australia.

1. Naniche D, Oldstone MB (2000) *Cell Mol Life Sci* 57:1399–1407.
2. Klenerman P, Hill A (2005) *Nat Immunol* 6:873–879.
3. Schneider-Schaulies S, Niewiesk S, Schneider-Schaulies J, ter Meulen V (2001) *Curr Mol Med* 1:163–181.
4. Zajac AJ, Blattman JN, Murali-Krishna K, Sourdive DJ, Suresh M, Altman JD, Ahmed R (1998) *J Exp Med* 188:2205–2213.
5. Wherry EJ, Blattman JN, Murali-Krishna K, van der Most R, Ahmed R (2003) *J Virol* 77:4911–4927.
6. Zinkernagel RM, Planz O, Ehl S, Battegay M, Odermatt B, Klenerman P, Hengartner H (1999) *Immunol Rev* 168:305–315.
7. Wu-Hsieh BA, Whitmire JK, de Fries R, Lin JS, Matloubian M, Ahmed R (2001) *J Immunol* 167:4566–4573.
8. Borrow P, Evans CF, Oldstone MB (1995) *J Virol* 69:1059–1070.
9. Odermatt B, Eppler M, Leist TP, Hengartner H, Zinkernagel RM (1991) *Proc Natl Acad Sci USA* 88:8252–8256.
10. Sevilla N, Kunz S, Holz A, Lewicki H, Homann D, Yamada H, Campbell KP, de La Torre JC, Oldstone MB (2000) *J Exp Med* 192:1249–1260.
11. Gretz JE, Kaldjian EP, Anderson AO, Shaw S (1996) *J Immunol* 157:495–499.
12. Bajenoff M, Egen JG, Koo LY, Laugier JP, Brau F, Glaichenhaus N, Germain RN (2006) *Immunity* 25:989–1001.
13. Cyster JG (2005) *Annu Rev Immunol* 23:127–159.
14. Wherry EJ, Ahmed R (2004) *J Virol* 78:5535–5545.
15. Van Vliet E, Melis M, Foidart JM, Van Ewijk W (1986) *J Histochem Cytochem* 34:883–890.
16. Macarak EJ, Howard PS, Lally ET (1986) *J Histochem Cytochem* 34:1003–1011.
17. Ahmed R, Hahn CS, Somasundaram T, Villarete L, Matloubian M, Strauss JH (1991) *J Virol* 65:4242–4247.
18. Matloubian M, Somasundaram T, Kolhekar SR, Selvakumar R, Ahmed R (1990) *J Exp Med* 172:1043–1048.
19. Matloubian M, Kolhekar SR, Somasundaram T, Ahmed R (1993) *J Virol* 67:7340–7349.
20. Gretz JE, Norbury CC, Anderson AO, Proudfoot AE, Shaw S (2000) *J Exp Med* 192:1425–1440.
21. Nolte MA, Belien JA, Schadee-Eestermans I, Jansen W, Unger WW, van Rooijen N, Kraal G, Mebius RE (2003) *J Exp Med* 198:505–512.
22. Oldstone MB, Sinha YN, Blount P, Tishon A, Rodriguez M, von Wedel R, Lampert PW (1982) *Science* 218:1125–1127.
23. Barber DL, Wherry EJ, Masopust D, Zhu B, Allison JP, Sharpe AH, Freeman GJ, Ahmed R (2006) *Nature* 439:682–687.
24. Sharpe AH, Wherry EJ, Ahmed R, Freeman GJ (2007) *Nat Immunol* 8:239–245.
25. Farr AG, Berry ML, Kim A, Nelson AJ, Welch MP, Aruffo A (1992) *J Exp Med* 176:1477–1482.
26. Sixt M, Kanazawa N, Selg M, Samson T, Roos G, Reinhardt DP, Pabst R, Lutz MB, Sorokin L (2005) *Immunity* 22:19–29.
27. Katakai T, Hara T, Sugai M, Gonda H, Shimizu A (2004) *J Exp Med* 200:783–795.
28. Kaldjian EP, Gretz JE, Anderson AO, Shi Y, Shaw S (2001) *Int Immunol* 13:1243–1253.
29. Benedict CA, De Trez C, Schneider K, Ha S, Patterson G, Ware CF (2006) *PLoS Pathog* 2:e16.
30. Durbeej M, Henry MD, Ferletta M, Campbell KP, Ekblom P (1998) *J Histochem Cytochem* 46:449–457.
31. Davis KJ, Anderson AO, Geisbert TW, Steele KE, Geisbert JB, Vogel P, Connolly BM, Huggins JW, Jahrling PB, Jaax NK (1997) *Arch Pathol Lab Med* 121:805–819.
32. Schacker TW, Brenchley JM, Beilman GJ, Reilly C, Pambuccian SE, Taylor J, Skarda D, Larson M, Douek DC, Haase AT (2006) *Clin Vaccine Immunol* 13:556–560.
33. Mueller SN, Jones CM, Smith CM, Heath WR, Carbone FR (2002) *J Exp Med* 195:651–656.